arXiv:1408.3662v1 [physics.plasm-ph] 15 Aug 2014

Separated spin-up and spin-down evolution of degenerated electrons in two dimensional systems: Dispersion of longitudinal collective excitations in plane and nanotube geometry

Pavel A. Andreev* and L. S. Kuz'menkov†
Faculty of physics, Lomonosov Moscow State University, Moscow, Russian Federation.
(Dated: August 19, 2014)

Applying the separated spin evolution quantum hydrodynamics to two-dimensional electron gas in plane samples and nanotubes located in external magnetic fields we find new kind of wave in electron gas, which is called the spin-electron acoustic wave. Separate spin-up electrons and spin-down electrons evolution reveals in replacement of the Langmuir wave by the couple of hybrid waves. One of two hybrid waves is the modified Langmuir wave. Another hybrid wave is the spin-electron acoustic wave. We study dispersion of these waves in two dimensional structures of electrons. We also consider dependence of dispersion properties on spin polarisation of electrons in external magnetic field.

The Langmuir wave is a fundamental process in multy electron three dimensional and low dimensional systems creating a background for many applications. Field of plasminics one of great examples of these applications. However, considering separate evolution of spin-up and spin-down electrons moving in an external magnetic field we find that collection of electrons reveals new collective excitation: the spin-electron acoustic wave [1]. This wave has been recently predicted and studied for three dimensional electron gas [1]. Properties of the spin-electron acoustic wave and modification of properties of the Langmuir wave in two dimensional electron gases (2DEGs) having plane and cylindric (nanotube) geometry is under theoretical consideration in this paper.

Carbone-nanotubes are most famous nanotubes, since they have been used in different application. However there are other types of nanotubes: gold [2], [3], [4], silicon-based [5], platinum [6] nanotubes, and MgO and Fe_3O_4-based nanostructures [7].

Hydrodynamic description of nanotubes can be found in Refs. [8]-[17]. π electron–hole plasma in single-walled metallic carbon nanotubes is considered in Ref. [18] in terms of two fluids hydrodynamics.

Carbone-nanotubes contain two types of electrons belonging to π and σ orbitals. They concentrations are different $n_{0\sigma} = 3n_{0\pi}$. That reveals in splitting of the Langmuir wave on two waves [19], [20]. This effect is described by the two liquid hydrodynamics, where electrons on π and σ orbitals are considered as different interacting species [19], [20].

In opposite to electron gas, electrons in graphite and carbone nanotubes are bounded to atoms. Three of four valence electrons are in strong σ bonds, and one electron occupies π orbital. At hybridisation of orbitals electrons occupy all for states with different modules and projection of the orbital momentum (one s state and three p states) having same spin projection. Thus valence electrons in carbone nanotubes are fully polarised. Since electrons of carbone nanotubes are fully polarised, we do not expect the spin-electron acoustic wave in carbone nanotubes.

Influence of spin on nanotubes properties have been recently discussed in Ref. [21]. Energy loss of a plasmon in a disorder-free carbon nanotube and plasmon decays into neutral bosonic excitations of the electron liquid were considered in Ref. [22].

Main tool of our research is the separated spin evolution quantum hydrodynamics (SSE-QHD) derived in Ref. [1]. The SSE-QHD is a generalisation of the spin-1/2 quantum hydrodynamics [23], [24], [25], [26]. Time evolution of the two dimensional particle densities (concentrations) n_u and n_d gives the continuity equations

$$\partial_t n_s + \nabla(n_s \mathbf{v}_s) = (-1)^{i_s} T_z, \tag{1}$$

where $s = \{u =\uparrow, d =\downarrow\}$, $[n_s] =\mathrm{cm}^{-2}$, $T_z = \frac{\gamma}{\hbar}(B_x S_y - B_y S_x)$ is the z-projection of torque presented in Cartesian coordinates, i_s: $i_u = 2$, $i_d = 1$, with the spin density projections S_x and S_y, each of them is a mix of $\psi_\uparrow$ and $\psi_\downarrow$, which are components of the wave spinor. Explicit form of S_x and S_y appear as $S_x = \psi^* \sigma_x \psi = \psi_d^* \psi_u + \psi_u^* \psi_d = 2a_u a_d \cos\Delta\phi$, $S_y = \psi^* \sigma_y \psi = \imath(\psi_d^* \psi_u - \psi_u^* \psi_d) = -2a_u a_d \sin\Delta\phi$, where $\Delta\phi = \phi_u - \phi_d$. These quantities do not related to different species of electrons having different spin direction. S_x and S_y describe simultaneous evolution of both species. Hence S_x and S_y do not wear subindexes u and d. We will apply the QHD equations for plane and cylindric geometries, but we have presented the torque in the Cartesian coordinates only, with no representation in the cylindrical coordinates. We have it done since it is a non-linear term. It does nor affect linear properties of electron gas, which are considered in this paper. We present some non-linear terms in the Euler equation, below, in the same manner. We note that $\mathbf{v} = \{v_x, v_y\}$ and $n = n(x, y)$, $\mathbf{v} = \mathbf{v}(x, y)$ for plane-like 2DEG, *and* $\mathbf{v} = \{v_\varphi, v_z\}$, and $n = n(\varphi, z)$, $\mathbf{v} = \mathbf{v}(\varphi, z)$ for nanotubes.

The time evolution of the particle currents for each

*Electronic address: andreevpa@physics.msu.ru
†Electronic address: lsk@phys.msu.ru

projection of spin $\mathbf{j}_u = n_u\mathbf{v}_u$ and $\mathbf{j}_d = n_d\mathbf{v}_d$ gives Euler equations

$$mn_s(\partial_t + \mathbf{v}_s\nabla)\mathbf{v}_s + \nabla p_s - \frac{\hbar^2}{2m}n_s\nabla\left(\frac{\triangle\sqrt{n_s}}{\sqrt{n_s}}\right)$$

$$= q_e n_s\left(\mathbf{E} + \frac{1}{c}[\mathbf{v}_s, \mathbf{B}]\right) + (-1)^{i_s}\frac{\gamma_e}{m}n_s\nabla B_z$$

$$+ \frac{\gamma_e}{2m}(S_x\nabla B_x + S_y\nabla B_y) + (-1)^{i_s}(\widetilde{\mathbf{T}}_z - m\mathbf{v}_s T_z), \quad (2)$$

with $\widetilde{\mathbf{T}}_z = \frac{\gamma_e}{\hbar}(\mathbf{J}_{(M)x}B_y - \mathbf{J}_{(M)y}B_x)$, which is the torque current, where

$$\mathbf{J}_{(M)x} = \frac{1}{2}(\mathbf{v}_u + \mathbf{v}_d)S_x - \frac{\hbar}{4m}\left(\frac{\nabla n_u}{n_u} + \frac{\nabla n_d}{n_d}\right)S_y, \quad (3)$$

and

$$\mathbf{J}_{(M)y} = \frac{1}{2}(\mathbf{v}_u + \mathbf{v}_d)S_y + \frac{\hbar}{4m}\left(\frac{\nabla n_u}{n_u} + \frac{\nabla n_d}{n_d}\right)S_x, \quad (4)$$

where $q_e = -e$, $\gamma_e = -g\frac{e\hbar}{2mc}$ is the gyromagnetic ratio for electrons, and $g = 1 + \alpha/(2\pi) = 1.00116$, where $\alpha = 1/137$ is the fine structure constant, so we include the anomalous magnetic moment of electrons. $\mathbf{J}_{(M)x}$ and $\mathbf{J}_{(M)y}$ are elements of the spin current tensor $J^{\alpha\beta}$. $\mathbf{J}_{(M)x}$, $\mathbf{J}_{(M)y}$, $\widetilde{\mathbf{T}}_z$, T_z are non-linear terms, and they do not give contribution in spectrum. p is the thermal pressure, or the Fermi pressure for degenerate fermions. Term proportional to the square of the Plank constant is the quantum Bohm potential.

The right-hand side of Euler equation present force fields of interaction. The first groups of terms in the right-hand side are the Lorentz forces. The second terms describe action of the z-projection of magnetic field on the magnetic moments (spins) of particles. Dependence on spin projection reveals in different signs before these terms. The third groups of terms in Euler equations contain a part of well-known force field $\mathbf{F}_S = M^\beta\nabla B^\beta$ describing action of the magnetic field on magnetic moments [23], [24]. Part of this force field has been presented by previous terms $\mathbf{F}_{S(z)} = \pm\gamma_e n_{u,d}\nabla B_z$. The second part of the force field $\mathbf{F}_{S(x,y)} = \gamma_e(S_x\nabla B_x + S_y\nabla B_y)$. The half of this force field enters each of the Euler equations. The last groups of terms is related to nonconservation of particle number with different spin-projection. This nonconservation gives extra mechanism for change of the momentum density revealing in the extra force fields.

At transition to the cylindric coordinates the inertia forces appear in hydrodynamic equations. These forces consist of three parts: the convective part (containing the velocity field $\mathbf{v}$), the thermal part (containing pressure p), and the quantum part (proportional to the square of the Planck constant $\hbar^2$). If the thermal pressure is isotropic, as we consider in this paper, the thermal pressure appears in the Euler equation in traditional form ∇p, with no extra terms. The convective part of the inertia forces gives no contribution in linear exitations on cylindric surface. The quantum part of the inertia forces together with the quantum part of the momentum flux tensor can be presented as the third term in equation (2). This form coincides with the traditional form of the quantum Bohm potential in Cartesian coordinates.

Spin evolution itself leads to new collective excitations [27]-[32], which are, some times, called the spin-plasma waves, but we do not consider them here.

We do not include influence of spin evolution on longitudinal waves. Thus we do not present equations for these quantities. These equations can be found in Ref. [1].

A model aimed to describe separated evolution of spin-up and spin-down electrons was considered in Ref. [33], but electrons with different spin projections are described there in the same manner as electrons with no spin separation. However it contradicts to the model directly derived from the Pauli equation, independently, for spin-up and spin-down electrons [1].

Electric and magnetic fields in the Euler equation (2) have the following explicit relation with sources of fields

$$\mathbf{E} = -q_e\nabla\int\frac{n_u + n_d - n_0}{\mid\mathbf{r} - \mathbf{r}'\mid}d\mathbf{r}', \quad (5)$$

and

$$\mathbf{B} = \int[(\mathbf{M}\nabla)\nabla - \mathbf{M}\triangle]\frac{1}{\mid\mathbf{r} - \mathbf{r}'\mid}d\mathbf{r}', \quad (6)$$

where $d\mathbf{r}'$ is a differential of two dimensional surface: $d\mathbf{r}' = dxdy$ for planes, and $d\mathbf{r}' = Rd\varphi dz$ for cylinders. n_0 in equation (5) presents motionless ions. $\mathbf{B} = \mathbf{B}(x, y)$, or $\mathbf{B} = \mathbf{B}(\varphi, z)$, and $\mathbf{B} = \{B_x, B_y, B_z\}$ or $\mathbf{B} = \{B_r, B_\varphi, B_z\}$, structure of $\mathbf{M}$ is similar to $\mathbf{B}$.

Equation of state for the pressure of spin-up $p_\uparrow$ and spin-down $p_\downarrow$ degenerate electrons, appears as $p_s = \pi\frac{\hbar^2}{m}n_s^2$. Pressure of spin-up electrons and spin-down electrons are different due to the external magnetic field, which changes an equilibrium concentration of each species $n_{0\uparrow} \neq n_{0\downarrow}$. In pressure p_s we have included that only one particle with a chosen spin direction can occupy one quantum state. As a consequence coefficient in the equation of state two times bigger than in the 2D Fermi pressure.

Equilibrium condition is described by the non-zero concentrations $n_{0\uparrow}$, $n_{0\downarrow}$, $n_0 = n_{0\uparrow} + n_{0\downarrow}$, and the external magnetic field $\mathbf{B}_{ext} = B_0\mathbf{e}_z$. Other quantities equal to zero $\mathbf{v}_{0\uparrow} = \mathbf{v}_{0\downarrow} = 0$, $\mathbf{E}_0 = 0$, $S_{0x} = S_{0y} = 0$. If we consider plane-like 2DEGs we place it in the plane $z = 0$, perpendicular to the external magnetic field. Hence waves propagate perpendicular to the external magnetic field. Perturbations of physical quantities are presented as $\delta f = F(\omega, k_x, k_y)e^{-\imath\omega t + \imath k_x x + \imath k_y y}$ and $k^2 = k_x^2 + k_y^2$, with $\delta f = \{\delta n_u, \delta n_d, \delta\mathbf{v}_u, \delta\mathbf{v}_d\}$. If we consider nanotubes we place them parallel to the external magnetic

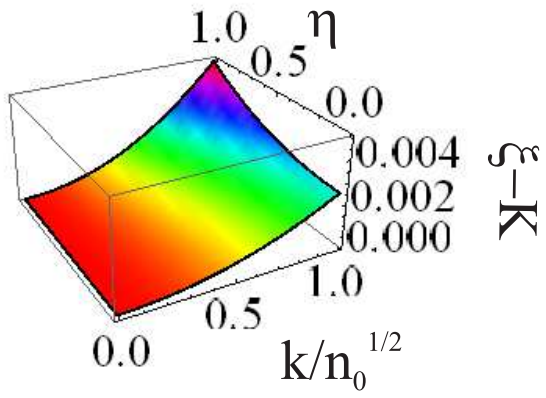

FIG. 1: (Color online) The figure shows dispersion of the Langmuir wave in plane-like 2DEGs and its dependence on spin-polarization. On this figure we use $\xi = \xi_{pl}$. Corresponding analytical solution is presented by formula (8) with plus before the square root.

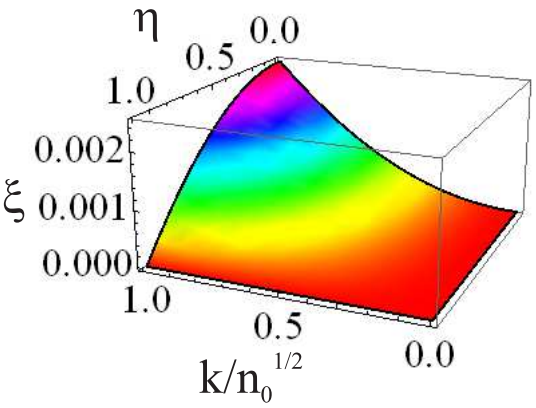

FIG. 2: (Color online) The figure shows dispersion and spin polarisation dependencies of the spin-electron acoustic wave for plane-like 2DEGs. On this figure we use $\xi = \xi_{pl}$. Corresponding analytical solution is presented by formula (8) with minus before the square root.

field. We present perturbations in the following form $\delta f = \int \sum_{l=0}^{\infty} F_l(k,\omega) e^{-\imath\omega t + \imath k z + \imath l\varphi} dk d\omega$. Representation of perturbations via exponents leads to sets of linear algebraic equations relatively to N_{Au}, N_{Ad}, V_{Au}, and V_{Ad}. Condition of existence of nonzero solutions for amplitudes of perturbations gives us a dispersion equation.

Difference of spin-up and spin-down concentrations of electrons $\Delta n = n_{0\uparrow} - n_{0\downarrow}$ is caused by external magnetic field. Since electrons are negative their spins get preferable direction opposite to the external magnetic field $\eta \equiv \frac{\Delta n}{n_0} = \tanh(\frac{\gamma_e B_0}{\varepsilon_{Fe,2D}}) = -\tanh(\frac{|\gamma_e| B_0}{\varepsilon_{Fe,2D}})$, where $\varepsilon_{Fe,2D} = \pi n_0 \hbar^2/m$, and $n_0 = n_{0u} + n_{0d}$.

We consider plasmas in the uniform constant external magnetic field. We see that in linear approach numbers of electrons of each species conserves.

Let us presents results for wave dispersion. We start with the plane-like 2DEG.

We assume that the external magnetic field is perpendicular to the plane, where the electron gas is located. Dispersion dependencies appears in the following form

$$\omega^2 - \Omega^2 = \frac{1}{2}\Bigg(\omega_{L,u}^2 + \omega_{L,d}^2 + (U_u^2 + U_d^2)k^2 \pm \Bigg[(\omega_{L,u}^2 + \omega_{L,d}^2)^2 + (U_u^2 - U_d^2)^2 k^4 + 2k^2(U_u^2 - U_d^2)(\omega_{L,u}^2 - \omega_{L,d}^2)\Bigg]^{1/2}\Bigg), \quad (7)$$

where $\omega_{L,s}^2 = 2\pi e^2 n_{0,s} k/m$ is the two dimensional Langmuir frequency for species s of electrons located in a plane, $\omega_L^2 = \omega_{L,u}^2 + \omega_{L,d}^2$ is the full Langmuir frequency, $\Omega = q_e B_0/(mc)$ is the cyclotron frequency, $U_s^2 = \frac{2\pi\hbar^2}{m^2} n_{0s} + \frac{\hbar^2 k^2}{4m^2}$ presents combined contribution of the Fermi pressure and the quantum Bohm potential.

Dropping the quantum Bohm potential and passing into dimensionless variables we obtain

$$\xi_{pl} = \frac{1}{2}\Big(K + \Lambda K^2 \pm \sqrt{K^2 + 2\Lambda K^3 \eta^2 + \Lambda^2 K^4 \eta^2}\Big), \quad (8)$$

where $\xi_{pl} = (\omega^2 - \Omega^2)/\omega_{ch}^2$, $K = k/\sqrt{n_0}$, $\Lambda = r_B\sqrt{n_0}$, with $\omega_{ch}^2 = 2\pi e^2 n_0^{\frac{3}{2}}/m$, $r_B = \hbar^2/(me^2)$ is the Bohr radius. Numerical analysis of formula (8) is presented on Figs. (1) and (2). The spin-electron acoustic wave (SEAW) exists at intermediate spin polarisation. It disappears at both the zero and full spin polarizations.

Fig. (1) shows the dimensionless shift of dispersion dependence of the Langmuir wave $\xi_{pl} - K$ from the Langmuir frequency square for 2DEG in plane ω_L^2. We note that 2D Langmuir frequency ω_L^2 is the linear function of the wave vector $k = K\sqrt{n_0}$. Fig. (1) depicts dependence of the shift $\xi_{pl} - K$ on the dimensionless wave vector K and spin polarisation η. We see that $\xi_{pl} - K$, as well as ξ_{pl}, increases with the increase of the wave vector. It happens due to the pressure of degenerate electron gas. Fig. (1) also shows that the growth of $\xi_{pl}(K)$ increases with increasing of the spin-polarisation. This effect appears due to dependence of pressure contribution on spin polarization via different occupation of quantum states by spin-up and spin-down electrons. We consider this effect by different pressure of spin-up and spin-down electrons. Nevertheless this effect can be included in single fluid model of electrons via corresponding equation of state (see Ref. [34] for more details).

Dispersion dependence of the SEAW $\xi_{pl}(K)$ at different spin polarisation η is depicted on Fig. (2). We see that frequency square of the SEAW $\xi_{pl}(K)$ on three orders smaller than the Langmuir frequency. We also see that frequency of the SEAW increases with the increase

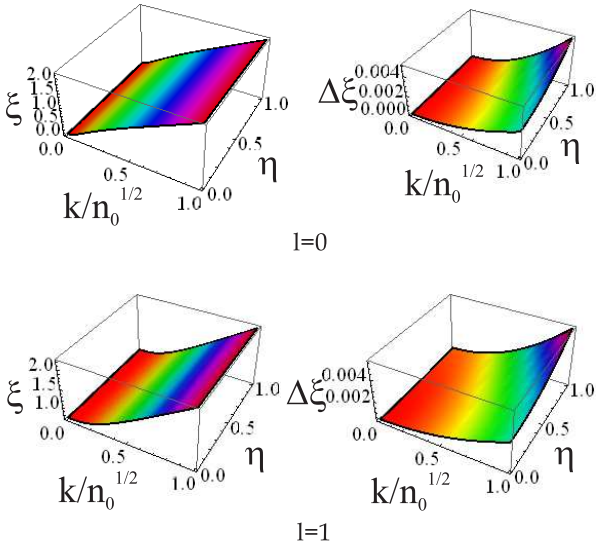

FIG. 3: (Color online) The figure shows dispersion of the Langmuir waves on cylindrical surface $\xi = \xi_{cyl}$ and shift of frequency square of the Langmuir waves $\Delta\xi$ from the Langmuir frequency square $\omega^2_{L,cyl}$ for $l = 0$ and $l = 1$. Analytical expression of dispersion is given by formula (11) with the plus before the square root.

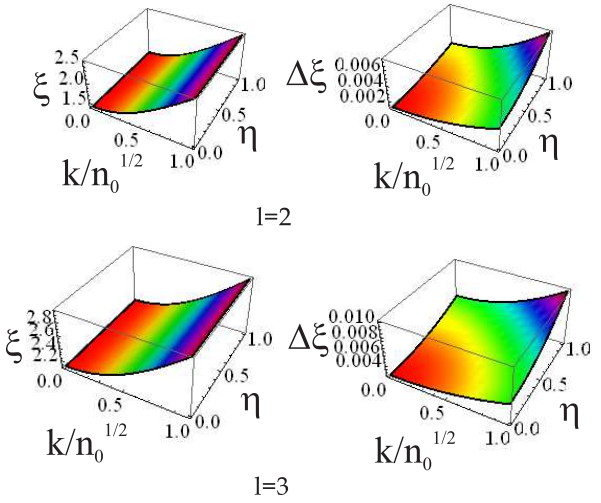

FIG. 4: (Color online) The figure shows dispersion of the Langmuir waves on cylindrical surface $\xi = \xi_{cyl}$ and shift of frequency square of the Langmuir waves $\Delta\xi$ from the Langmuir frequency square $\omega^2_{L,cyl}$ for $l = 2$ and $l = 3$. Analytical expression of dispersion is given by formula (11) with the plus before the square root.

of the wave vector k. The rate of the increasing slows down with growth of the spin polarisation.

We present now results for 2DEG on the cylindric surface.

External magnetic field is parallel to the axis of the cylinder (nanotube), where electron gas is located. Cor-

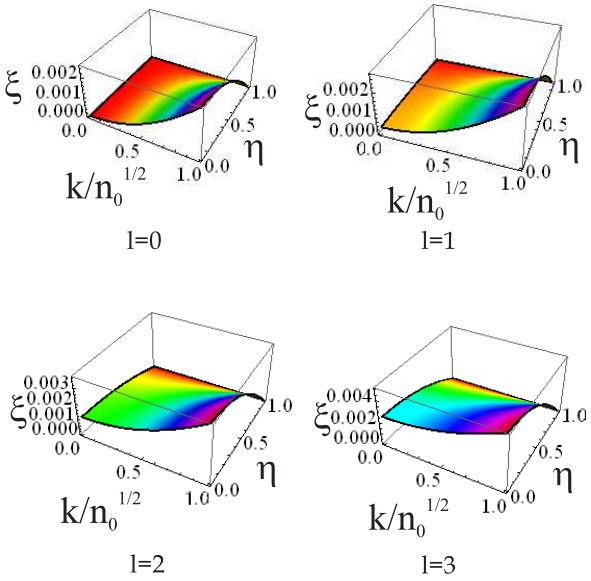

FIG. 5: (Color online) The figure presents spectrums of the spin-electron acoustic wave at different values of discrete wave number $k_\varphi = l/R$. We present dispersion surfaces for l =0, 1, 2, 3. Analytical expression of dispersion is given by formula (11) with the minus before the square root.

responding dispersion dependence appears as

$$\omega^2 = \frac{1}{2}\Bigg(\omega^2_{L,cyl} + \frac{l^2}{R^2}\left[v_u^2 + v_d^2 + \frac{\hbar^2}{2m^2}\left(k^2 + \frac{l^2+2}{R^2}\right)\right]$$

$$+k^2\left[v_u^2 + v_d^2 + \frac{\hbar^2}{2m^2}\left(k^2 + \frac{l^2}{R^2}\right)\right]$$

$$\pm\Bigg[\left(k^2 + \frac{l^2}{R^2}\right)^2[v_u^2 - v_d^2 + e^2RG(n_{0u} - n_{0d})/m]^2$$

$$+ 4\omega^2_{L,cyl,u}\omega^2_{L,cyl,d}\Bigg]^{1/2}\Bigg), \qquad (9)$$

where

$$\omega^2_{L,cyl,s} = \frac{Ge^2n_{0,s}}{m}R\left(k^2 + \frac{l^2}{R^2}\right), \qquad (10)$$

is the Langmuir frequency of electron gas on the cylinder for species $s = \{u = \uparrow, d = \downarrow\}$ of electrons, $\omega^2_{L,cyl} = \omega^2_{L,cyl,u} + \omega^2_{L,cyl,d}$ is the full Langmuir frequency, $v_s^2 = 2\pi\hbar^2 n_{0s}/m^2$ presents contribution of the Fermi pressure, and $G = G(R,k,l) = 4\pi I_l(kR)K_l(kR)$, with $I_l(x)$, $K_l(x)$ are the modified Bessel functions.

Dimensionless form of dispersion dependence (9) can be written as

$$\xi_{cyl} = \frac{1}{2}\left(K^2 + l^2Y^2\right)\left(\frac{G}{2\pi Y} + \Lambda\right.$$

$$\pm\sqrt{\left(\frac{G}{2\pi Y}\right)^2+2\eta^2\frac{G}{2\pi Y}\Lambda+\eta^2\Lambda^2}\Bigg), \qquad (11)$$

where $\xi_{cyl}=\omega^2/\omega_{ch}^2$, $K=k/\sqrt{n_0}$, $\Lambda=r_B\sqrt{n_0}$, $Y=1/(R\sqrt{n_0})$.

Figs. (3) and (4) show behavior of the Langmuir wave dispersion in 2DEG on the cylindric surface. At numerical analysis we assume that radius of the cylinder equal 30 nm. At $l=0$ frequency square of the Langmuir wave ξ almost linearly depends on the wave vector k, but frequency shift $\Delta\xi=\xi-\omega_{Le,cyl}^2(k,l)/\omega_{ch}^2$ shows small difference from the linear growth. This difference is related to the pressure of degenerate gas. We also see that the pressure contribution dependes on spin polarisation η. At $l\neq 0$, $\xi(k)$ reveals almost parabolic dependence due to structure of the Langmuir frequency square for electron gas on the cylindric surface.

Increase of the discrete wave number $k_\varphi=l/R$ gives an increase of whole dispersion surface. At the same time, the increase of l leads to increase of the shift $\Delta\xi(K,\eta)$. Form of surfaces describing the shift $\Delta\xi(K,\eta)$ also changes with increasing of l: area of small wave numbers and large spin polarisation grows up faster than other areas.

Fig. (5) describes the SEAW in the cylindric 2DEG for l=0, 1, 2, 3. General behavior shows resemblance to dispersion of the SEAW in plane-like 2DEG: increase of $\xi(k)$, lowering of $\xi(k)$ with increasing of spin polarisation η. Increasing of l reveals in modification of dispersion surface of the SEAW. Values of ξ increase with the increase of l. Moreover, the area of small wave vectors and small spin polarisation increases relatively faster. Modifications of ξ_{cyl} for the SEAW and $\Delta\xi_{cyl}$ for the Langmuir wave happening with the change of l are different. Different areas of these surfaces show relative growth. In both cases these areas are located at small wave vectors. However they are located at different values of the spin polarisation η. Relative increase of $\Delta\xi_{cyl}$ for the Langmuir wave is at large η. Whereas, the relative increase of ξ_{cyl} for the SEAW is at small spin polarisation η.

In this paper we have discussed increase of frequency of the 2D Langmuir excitations due to different occupation of spin-up and spin-down states in the electron gas located in the external magnetic field. We have demonstrated existence of the SEAW in 2D structures (planes and nanotubes). We have described properties of the SEAW. These results have been obtained by means of the SSE-QHD.

[1] P. A. Andreev, arXiv:1405.0719.
[2] Jian Zhou and Jinming Dong, Phys. Rev. B **75**, 155423 (2007).
[3] D. Zs. Manrique, J. Cserti, and C. J. Lambert, Phys. Rev. B **81**, 073103 (2010).
[4] Jesse Kohl, Micha Fireman, and Deirdre M. O'Carroll, Phys. Rev. B **84**, 235118 (2011).
[5] Gian G. Guzman-Verri, L. C. Lew Yan Voon, Phys. Rev. B **76**, 075131 (2007).
[6] Shyamal Konar and Bikash C. Gupta, Phys. Rev. B **78**, 235414 (2008).
[7] J. Mejia-Lopez, J. Mazo-Zuluaga, S. Lopez-Moreno, F. Munoz, L. F. Duque, and A. H. Romero, Phys. Rev. B **90**, 035411 (2014).
[8] P. Longe and S. M. Bose, Phys. Rev. B **48**, 18239 (1993).
[9] C. Yannouleas, E. N. Bogachek, and U. Landman, Phys. Rev. B **50**, 7977 (1994).
[10] Constantine Yannouleas, Eduard N. Bogachek, and Uzi Landman, Phys. Rev. B **53**, 225 (1996).
[11] Xudong Jiang, Phys. Rev. B **54**, 487 (1996).
[12] D. J. Mowbray, S. Segui, J. Gervasoni, Z. L. Miskovic, and N. R. Arista, Phys. Rev. B **82**, 035405 (2010).
[13] Christoph Schenke, Sonja Koller, Leonhard Mayrhofer, and Milena Grifoni, Phys. Rev. B **80**, 035412 (2009).
[14] Afshin Moradi, Physics of Plasmas **17**, 014504 (2010).
[15] Afshin Moradi, J. Phys.: Condens. Matter **21**, 045303 (2009).
[16] Li Wei, You-Nian Wang, Phys. Rev. B **75**, 193407 (2007).
[17] S. A. Khan and Sunia Hassan, Journal of Applied Physics **115**, 204304 (2014).
[18] Afshin Moradi, Physics Letters A **372**, 5614 (2008).
[19] Afshin Moradi, and Heidar Khosravi, Phys. Rev. B **76**, 113411 (2007).
[20] S. Dmitrovic, T. Vukovic, B. Nikolic, M. Damnjanovic, and I. Milosevic, Phys. Rev. B **77**, 245415 (2008).
[21] Andras Palyi, P. R. Struck, Mark Rudner, Karsten Flensberg, and Guido Burkard, Phys. Rev. Lett. **108**, 206811 (2012).
[22] Wei Chen, A. V. Andreev, E. G. Mishchenko, L. I. Glazman, Phys. Rev. B **82**, 115444 (2010).
[23] T. Takabayasi, Prog. Theor. Phys. **13**, 222 (1955); T. Takabayasi, Prog. Theor. Phys. **14**, 283 (1955).
[24] L. S. Kuz'menkov, S. G. Maksimov, and V. V. Fedoseev, Theor. Math. Fiz. **126** 136 (2001) [Theoretical and Mathematical Physics, **126** 110 (2001)].
[25] M. Marklund and G. Brodin, Phys. Rev. Lett. **98**, 025001 (2007).
[26] P. A. Andreev and L. S. Kuz'menkov, Russian Phys. Jour. **50**, 1251 (2007).
[27] P. A. Andreev, L. S. Kuz'menkov, Moscow University Physics Bulletin **62**, N.5, 271 (2007).
[28] G. Brodin, M. Marklund, J. Zamanian, B. Ericsson and P. L. Mana, Phys. Rev. Lett. **101**, 245002 (2008).
[29] A. P. Misra, G. Brodin, M. Marklund and P. K. Shukla, J. Plasma Physics **76**, 857 (2010).
[30] P. A. Andreev, L. S. Kuz'menkov, Int. J. Mod. Phys. B **26** 1250186 (2012).
[31] M. I. Trukhanova, Prog. Theor. Exp. Phys., 111I01 (2013).
[32] P. K. Shukla, B. Eliasson, Rev. Mod. Phys. **83**, 885 (2011).
[33] G. Brodin, A. P. Misra, and M. Marklund, Phys. Rev. Lett. **105**, 105004 (2010).
[34] P. A. Andreev, Annals of Physics **350**, 198 (2014).